Combinatorial Screening of Complex Block Copolymer Assembly with Self-Consistent Field Theory

François Drolet and Glenn H. Fredrickson

*Department of Chemical Engineering and Materials Research Laboratory, University of California,
Santa Barbara, California 93106*

We describe a numerical implementation of self-consistent mean field theory for block copolymers that requires no assumption of the mesophase symmetry. The method is amenable to massively parallel screening of self-assembly in complex block copolymer systems, characterized by high-dimensional parameter spaces. We illustrate the method by screening for novel mesophases in linear *ABCA* tetrablock copolymers; several previously unreported mesophases have been identified. Extension to multicomponent systems, such as blends of block copolymers and homopolymers, is straightforward.

Computational materials discovery and design has long been the dream of materials technologists. To date, however, the discovery phase for most new materials is driven largely by experimental programs, with theoreticians struggling to explain structures and phenomena after they have been observed in the laboratory. Among soft materials, block copolymers are unique in that a quantitative theory is available for relating molecular architecture and composition to equilibrium self-assembly [1]. This theory, a type of self-consistent mean field theory (SCMFT), has been extraordinarily successful in helping to explain the complex mesophases experimentally observed in block copolymers and polymer alloys [2].

SCMFT for polymer melts has its origins in work by Edwards in the 1960s and was explicitly adapted to treat block copolymer self-assembly by Helfand and others in the subsequent decades [3]. The current state-of-the-art numerical approach to solving the SCMFT equations is due to Matsen and Schick and involves expanding all spatially dependent fields in a finite set of basis functions with an *assumed* mesophase symmetry [2,4]. While the Matsen-Schick approach is numerically efficient and allows high precision calculations of free energies and phase diagrams, the requirement of a symmetry assumption makes it unsuitable for the discovery of previously unknown mesophases in complex copolymer melts. In the present Letter, we describe an alternative numerical approach to solving the SCMFT equations that lends itself to combinatorial screening of new mesophases in block copolymer systems.

To explain the need for such a tool, it is helpful to review the rapid expansion of parameter space and richness of self-assembly behavior that is observed as block copolymers are composed with increasing numbers of chemically distinct blocks (polymerized sequences of like monomers) [1]. The equilibrium phase behavior of simple *AB* diblock copolymers is dictated in SCMFT by two parameters: $h_{AB} = \chi_{AB} N$, where χ_{AB} is a binary interaction parameter ("Flory parameter") between dissimilar monomers and N is the overall number of monomers per chain, and f_A, the volume fraction of the *A* block of each molecule. In this two-dimensional parameter space, four spatially periodic mesophases (lamellae, hexagonally packed cylinders, bcc spheres, and the "gyroid" phase $-Ia\bar{3}d$ space group) have been experimentally observed and theoretically confirmed via the Matsen-Schick algorithm [5]. For the case of linear polymers with three chemically distinct blocks, i.e., *ABC* triblocks, the parameter space for SCMFT is five-dimensional (h_{AB}, h_{AC}, h_{BC}, f_A, f_B) and over 13 distinct mesophases have been experimentally identified to date [1,6]. By switching from the linear *ABC* architecture to the *ABC star* architecture, additional fascinating mesophase symmetries have recently been identified [7]. Evidently, as the number of distinct blocks and possibilities for block connectivity grow, there is a dramatic expansion in the number and types of self-assembled mesophases, as well as explosive growth in the parameter space that must be explored to unearth these phases. A theoretical tool for "combinatorial screening" of self-assembly in such complex systems would evidently be very useful.

Here we present an algorithm for implementing SCMFT that can serve as such a screening tool. For concreteness, we restrict attention to a linear *ABCDE*··· multiblock melt, where each chain has *M* distinct blocks and a total of *N* monomers, and adopt the notation of Matsen and Schick [4]. In mean field theory, each such chain has independent statistics in average chemical potential fields, $w_K(\mathbf{r})$, conjugate to the volume fraction fields, $\phi_K(\mathbf{r})$, of block species *K*. The free energy per chain (in units of $k_B T$) is given by [4]

$$
\begin{aligned}
F = &-\ln[V^{-1} \int d\mathbf{r}\, q(\mathbf{r}, 1)] \\
&+ [1/(2V)] \sum_{K \neq} \sum_L h_{KL} \int d\mathbf{r}\, \phi_K \phi_L \\
&- (1/V) \sum_K \int d\mathbf{r}\, w_K \phi_K .
\end{aligned} \tag{1}
$$

The function $q(\mathbf{r}, s)$ is the statistical weight that a segment of a chain, originating from the free end of the A block and with contour length s, has at its terminus at point $\mathbf{r}$. The contour variable s is scaled by N and lengths have been scaled by the unperturbed radius of gyration of the chain, R_g. V is the system volume expressed in these units and $q(\mathbf{r}, 1)$ is the statistical weight of a constrained end of an entire chain.

The above free energy expression is to be minimized subject to the constraint of local incompressibility, $\sum_K \phi_K(\mathbf{r}) = 1$, and the constraint that $q(\mathbf{r}, s)$ satisfies a dynamical trajectory given by the solution of $\partial_s q = \nabla^2 q - w(\mathbf{r}, s)q$, $q(\mathbf{r}, 0) = 1$. The latter constraint is a Feynman-Kac formula for the single chain path integral; the function $w(\mathbf{r}, s)$ is defined as $w_K(\mathbf{r})$, for all s on blocks of species K. Imposition of these constraints leads naturally to two Lagrange multiplier fields: a pressure field $P(\mathbf{r})$ and a conjugate statistical weight $q^\dagger(\mathbf{r}, s)$ satisfying $-\partial_s q^\dagger = \nabla^2 q^\dagger - w(\mathbf{r}, s)q^\dagger$, $q^\dagger(\mathbf{r}, 1) = 1$. $q^\dagger(\mathbf{r}, s)$ gives the statistical weight of a (conjugate) segment of chain that has its terminal end at position $\mathbf{r}$ and contour location s, and the other end ($s = 1$) distributed throughout the entire volume. Minimization with respect to $\phi_K(\mathbf{r})$ and $w_K(\mathbf{r})$ leads to the following equations that complete the SCMFT set:

$$w_K(\mathbf{r}) = \sum_{L \neq K} h_{KL}\phi_L(\mathbf{r}) + P(\mathbf{r}), \qquad (2)$$

$$\phi_K(\mathbf{r}) = V \int ds\, q(\mathbf{r}, s)q^\dagger(\mathbf{r}, s) \Big/ \left[\int d\mathbf{r}\, q(\mathbf{r}, 1) \right], \quad (3)$$

where the chain contour integral on s is restricted to blocks of species K.

Matsen and Schick [4] solve the above equations by using a restricted Fourier basis appropriate for an assumed mesophase symmetry. Our approach is to search for low free energy solutions of the equations by solving the equations in real space within a box with periodic boundary conditions. So as not to bias the symmetry of patterns that emerge, this optimization is carried out starting with randomly generated potential fields. While other groups [8,9] also employ a real-space approach to SCMFT, our goals are rather different. In particular, we consider bulk melts, rather than thin films. Moreover, the algorithm is not intended to mimic real polymer dynamics, but is simply an artifice to evolve a system as rapidly as possible to a free energy minimum satisfying the above constraints (including rigorous incompressibility). We expect that this will prove to be a particularly efficient methodology for screening of block copolymer self-assembly.

A sketch of our Picard-type algorithm is as follows. First, an initial guess for the $w_K(\mathbf{r})$ is constructed with a random number generator. Equation (2) is then combined with the condition of incompressibility to solve for the fields $\phi_K(\mathbf{r})$ and $P(\mathbf{r})$. Using a Crank-Nicholson scheme, the diffusion equations are then integrated to obtain q and $q^\dagger$ for $0 \leq s \leq 1$. Next, the right-hand side of

Eq. (3) is evaluated to obtain new expressions for the species volume fractions. The volume fractions at the next iteration are obtained by means of a linear mix of new and old solutions. The final step is to update the potential fields using Eq. (2) and subsequently update the pressure field by combining Eq. (2) with the condition of incompressibility. These steps are repeated until the free energy changes at each iteration are reduced to 10^{-4}, or until the pattern emerging in the simulation box can be clearly identified. The structures so obtained correspond to either stable or metastable equilibrium. In principle, one can assess the relative stability of competing mesophases by comparing their free energies. Each independent run, starting from a different random initial condition, can be viewed as a quench. Quenches in different regions of parameter space are statistically independent and are amenable to parallel computation.

As an example, we show in Fig. 1 results from two independent quenches in a study of AB diblock copolymer melts performed with $h_{AB} = 16$. The simulation box was a two-dimensional square 128×128 grid with side length $L \equiv V^{1/2} = 10$ (in units of R_g). In such a two-dimensional calculation it is possible to resolve mesophases with composition variations in up to two directions; this clearly excludes intrinsically three-dimensional mesophases such as the cubic bcc and gyroid structures. If the value of L is too small, the mesophase emerging in the box is highly constrained by the periodic cell. On the other hand, excessively large values of L slow the equilibration process as defects must be annealed out over large distances. In practice, L is initially chosen to be a small multiple of R_g, e.g., $L = 5$, and is then increased until the changes in free energy are below some threshold. The volume fraction of the A block of each molecule was set to $f_A = 0.5$ for the left column of Fig. 1 and $f_A = 0.67$ for the right column. The three configurations displayed in each column illustrate how the A-monomer volume fraction changes in our algorithm as a minimum of the free energy is approached. The bottom row of the figure shows the final configuration obtained in each case. These are consistent with the lamellar and cylindrical phases expected from the phase diagram of Matsen and Schick [4]. In fact, we have confirmed that the above algorithm, when implemented in *three dimensions* for AB diblock copolymers, leads to equilibrated lamellar, cylindrical, cubic, and gyroid mesophases at compositions and h_{AB} values consistent with the Matsen-Schick phase diagram. In a few instances, we arrived at the perforated lamellar phase, which is known to be metastable [4,5,10], but is nonetheless experimentally observed [11]. Repetition of these quenches using the same parameters, but different random initial conditions, confirmed that this phase was not robust.

As a first application of our approach to combinatorial screening of mesophases in a new system, we have examined linear $ABCA$ tetrablock copolymers. This
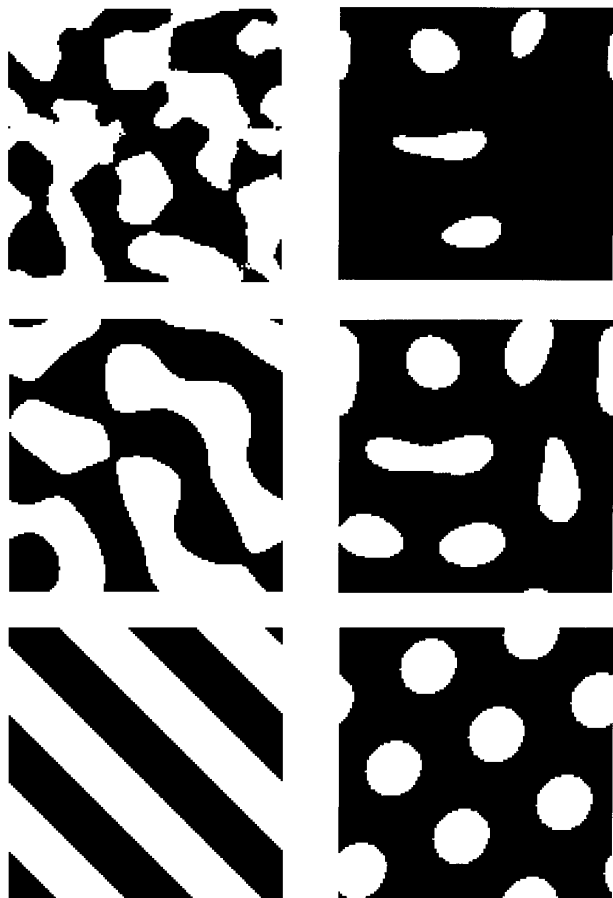
FIG. 1. Microphase separation in a two-dimensional melt of AB diblock copolymers with $h_{AB} = 16$ and $f_A = 0.5$ (left column) and $f_A = 0.67$ (right column). In both cases, the algorithm described in the text leads to the proper equilibrium mesophase (lamellar and cylindrical phases, respectively). Regions rich in A monomers are shown in black.

architecture differs from the well-studied ABC architecture in that A is covalently bonded to both B and C, which produces an additional source of frustration not present in ABC melts. Thus, we might expect to see new types of self-assembly. Practical interest in such systems could involve applications as thermoplastic elastomers, where A is a glassy or crystalline hard polymer, and B and C are rubbery blocks capable of microphase separation. The possibility of complex geometrical structuring of the rubbery blocks in such materials could lead to novel stress-strain characteristics.

Even with the restriction of equal-volume A blocks, the parameter space of an $ABCA$ melt in SCMFT is five-dimensional (h_{AB}, h_{AC}, h_{BC}, f_B, f_C), so exhaustive exploration of this space for new types of self-assembly is a formidable task. To reduce the labor involved, we have restricted our screening to two-dimensional patterns (spatial variation in only two directions) and have set $h_{AB} = h_{AC} = h_{BC}$. Undoubtedly, these restrictions have caused us to miss a number of interesting mesophase struc-

tures. Nevertheless, our screening, which consisted of 500 independent quenches distributed throughout the above parameter space, has unearthed several new mesophase structures.

We start with a description of the various types of self-assembly we have encountered by varying f_A while keeping $f_B = f_C$. At small values of f_A, the tetrablocks microphase separate into B-rich and C-rich lamellae. A monomers from the first (last) block of the $ABCA$ architecture locate preferentially inside the B-rich (C-rich) phase. The overall density of A monomers, however, is largest in the interfacial region. In fact, when f_A is increased above approximately 0.25, small A decorations form at regular intervals along the B-C interfaces [Fig. 2(a)]. Their location along neighboring interfaces is staggered, leading to a pattern with $p2mg$ symmetry. At nearly equal volume fractions of the three species ($f_A = 0.34, f_{B,C} = 0.33$), the melt self-assembles into a hexagonal phase [Fig. 2(b)]. The same morphology was recently observed in three-dimensional Monte Carlo simulations of ABC *star-block* copolymers [12], but has not been previously hypothesized for the $ABCA$ architecture or experimentally observed in any copolymer system to date. It is interesting to note that for the same parameter values, our simulations of
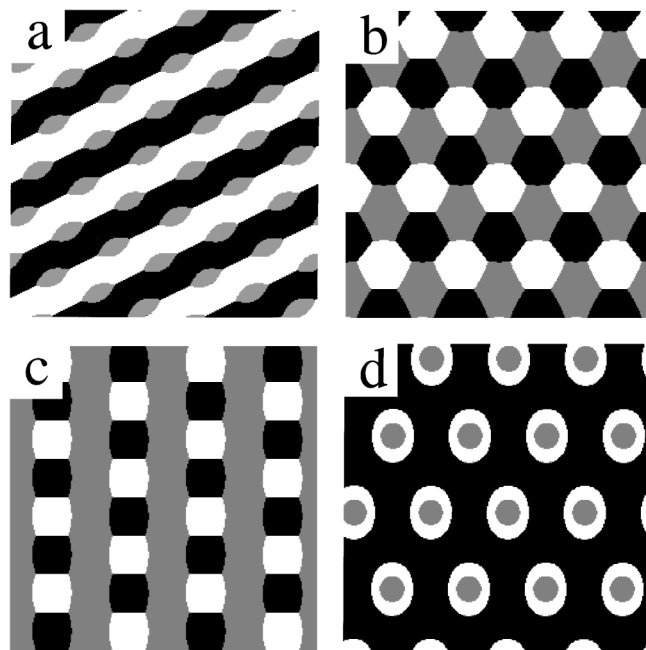

FIG. 2. Examples of mesophases obtained by solving the SCMFT equations for $ABCA$ tetrablock melts on a 128×128 square lattice. Regions rich in A, B, or C monomers are shown in grey, black, and white, respectively. In all four cases, we used $h_{AB} = h_{AC} = h_{BC} = 35$ and replicated the final pattern 4 times to form the configurations shown above. (a) $f_A = 0.26$, $f_{B,C} = 0.37$, and $L = 7$, where L is the length of each side of the simulation box in units of R_g. (b) $f_A = 0.34$, $f_{B,C} = 0.33$, and $L = 5$. (c) $f_A = 0.48$, $f_{B,C} = 0.26$, and $L = 5$. (d) $f_A = 0.24$, $f_B = 0.56$, $f_C = 0.20$, and $L = 7$.

ABC linear triblocks readily produced the "three-color" (*ABCCBA*···) lamellar phase, which has been observed in a number of experiments on *ABC* systems [6]. The *ABCA* architecture in our experience is apparently much less inclined to form three-color lamellae.

For $0.4 < f_A < 0.6$ and $f_B = f_C$, we have observed a mesophase that consists of long, parallel chains of alternating *B*-rich and *C*-rich "beads" embedded in a matrix of A [Fig. 2(c)]. Beads rich in one species on one chain face beads rich in the other on the neighboring chains. We are not aware of any previous predictions or observation of this "bead phase" (plane group $c2mm$) in block copolymers of any architecture. Finally, for values of f_A in the interval $0.6 < f_A < 0.74$ and equal $f_{B,C}$, *B* and *C* monomers uniformly mix inside small disks arranged on a triangular lattice within the continuous *A* matrix. This phase is the analog of the familiar hexagonal *B*-cylinder phase in *AB* diblock copolymers.

Quenches in regions of parameter space with $f_B \neq f_C$ have yielded one additional interesting microstructure that is shown in Fig. 2(d) ($f_A = 0.24, f_B = 0.56, f_C = 0.20$). This is a core-shell cylindrical phase similar to that observed in *ABC* linear triblocks. In the present case, however, the *A*-rich phase at the center of each disk consists mainly of *A* monomers from the last block of the *ABCA* chains. The density of *A* monomers from the first block is largest just outside the *C*-rich annular regions and slowly decays into the *B*-rich matrix. (These *A* monomers are never in the majority anywhere in the structure, but are mixed into the black *B* region.) The disks in Fig. 2(d) are slightly elongated in the vertical direction due to the constraints of the periodic box with $L = 7$. We have confirmed that quenches with larger values of L restore a circular shape to the disks, but at the cost of dramatically increased run time to anneal out defects in the structure.

In summary, we have developed a real-space approach to implementing polymer SCMFT that is particularly well suited to screening for new types of self-assembly in complex block copolymer systems. By performing a large number of parallel quenches distributed throughout the parameter space of interest, it is possible to construct a set of candidate spatially periodic mesophases that may represent either stable or metastable structures. Given this candidate set of structures, the Matsen-Schick algorithm is then ideally suited for the accurate calculation of free energies and construction of phase diagrams. We believe that this tandem approach to implementing SCMFT will prove to be extremely effective in sorting out the complexities of self-assembly in multiple-color block copolymer systems and invaluable in guiding experimentation. In closing, we emphasize that the approach is very general and can be easily extended to essentially any block architecture and to include additional components, such as solvents or homopolymers.

[1] F. S. Bates and G. H. Fredrickson, Phys. Today **52**, No. 2, 32 (1999).

[2] M. W. Matsen and M. Schick, Curr. Opin. Colloid Interface Sci. **1**, 329 (1996).

[3] S. F. Edwards, Proc. Phys. Soc. **85**, 613 (1965); E. Helfand, J. Chem. Phys. **62**, 999 (1975); E. Helfand and Z. R. Wasserman, Macromolecules **9**, 879 (1976); K. M. Hong and J. Noolandi, *ibid.* **14**, 727 (1981); J. D. Vavasour and M. D. Whitmore, *ibid.* **25**, 5477 (1992).

[4] M. W. Matsen and M. Schick, Phys. Rev. Lett. **72**, 2660 (1994).

[5] M. W. Matsen and F. S. Bates, Macromolecules **29**, 1091 (1996).

[6] R. Stadler *et al.,* Macromolecules **28**, 3080 (1995); K. Jung, V. Abetz, and R. Stadler, *ibid.* **29**, 1076 (1996); Y. Mogi *et al., ibid.* **27**, 6755 (1994); G. Riess *et al.,* J. Macromol. Sci. Phys. B **17**, 335 (1980).

[7] S. Sioula, N. Hadjichristidis, and E. L. Thomas, Macromolecules **31**, 5272 (1998); **31**, 8429 (1998).

[8] B. A. C. van Vlimmeren *et al.,* Macromolecules **32**, 646 (1999); J. G. E. M. Fraaije *et al.,* J. Chem. Phys. **106**, 4260 (1997).

[9] G. T. Pickett and A. C. Balazs, Macromol. Theory Simul. **7**, 249 (1998); K. R. Shull, Macromolecules **26**, 2346 (1993).

[10] S. Qi and Z.-G. Wang, Phys. Rev. E **55**, 1682 (1997).

[11] I. W. Hamley *et al.,* Macromolecules **26**, 5959 (1993).

[12] T. Dotera and A. Hatano, J. Chem. Phys. **105**, 8413 (1996).